Check for updates

UGT1A3 and Sex Are Major Determinants of Telmisartan Pharmacokinetics—A Comprehensive Pharmacogenomic Study

Päivi Hirvensalo[1,2], Aleksi Tornio[1,2], Terhi Launiainen[1,2], Maria Paile-Hyvärinen[1,2], Tuija Tapaninen[1,2], Mikko Neuvonen[1,2], Janne T. Backman[1,2] and Mikko Niemi[1,2,*]

To investigate how variability in multiple pharmacokinetic genes associates with telmisartan exposure, we determined telmisartan single-dose (40 mg) pharmacokinetics and sequenced 379 genes in 188 healthy volunteers. Intronic *UGT1A* variants showed the strongest associations with the area under the plasma concentration-time curve from zero hours to infinity ($AUC_{0-\infty}$) and peak plasma concentration (C_{max}) of telmisartan. These variants were strongly linked with the increased function *UGT1A3*2* allele, suggesting that it is the causative allele underlying these associations. In addition, telmisartan plasma concentrations were lower in men than in women. The *UGT1A3*2* was associated with a 64% and 63% reduced $AUC_{0-\infty}$ of telmisartan in *UGT1A3*2* heterozygous and homozygous men, respectively ($P = 1.21 \times 10^{-16}$ and 5.21×10^{-8}). In women, *UGT1A3*2* heterozygosity and homozygosity were associated with 57% ($P = 1.54 \times 10^{-11}$) and 72% ($P = 3.31 \times 10^{-15}$) reduced $AUC_{0-\infty}$, respectively. Furthermore, a candidate gene analysis suggested an association of *UGT1A3*3* and the *SLCO1B3* c.767G>C missense variant with telmisartan pharmacokinetics. A genotype score, which reflects the effects of sex and genetic variants on telmisartan $AUC_{0-\infty}$, associated with the effect of telmisartan on diastolic blood pressure. These data indicate that sex and UGT1A3 are major determinants and suggest a role for OATP1B3 in telmisartan pharmacokinetics.

Study Highlights

WHAT IS THE CURRENT KNOWLEDGE ON THE TOPIC?

☑ High interindividual variability exists in the pharmacokinetics of telmisartan. There are no comprehensive studies evaluating how variability in multiple pharmacokinetic genes associates with telmisartan exposure.

WHAT QUESTION DID THIS STUDY ADDRESS?

☑ This study investigated how genetic variants associate with telmisartan single-dose pharmacokinetics in healthy volunteers.

WHAT THIS STUDY ADD TO OUR KNOWLEDGE?

☑ This study shows that the *UGT1A3*2* and **3* alleles are associated with reduced telmisartan exposure and the *SLCO1B3* c.767G>C missense variant with increased telmisartan exposure. Based on the results, genotype scores were generated to predict telmisartan pharmacokinetics in men and women with different combinations of *UGT1A3* and *SLCO1B3* variants.

HOW THIS MIGHT CHANGE CLINICAL PHARMACOLOGY OR TRANSLATIONAL SCIENCE?

☑ This knowledge might aid in identifying individuals with increased risk of insufficient telmisartan exposure and impaired blood pressure-lowering response with the 40 mg dose. This may aid in individualizing antihypertensive therapy.

Telmisartan is an angiotensin II receptor antagonist for treatment of hypertension.[1] Uridine diphosphate-glucuronosyltransferase (UGT) 1A3 metabolizes telmisartan extensively to an acyl-glucuronide metabolite, which is the only telmisartan metabolite found in humans.[2,3] UGT1A1, 1A7, 1A8, and 1A9 may also contribute to telmisartan glucuronidation.[3] Furthermore, *in vitro* studies have suggested the involvement of OATP1B3 (encoded by *SLCO1B3*) and 2B1 (encoded by *SLCO2B1*) transporters in the cellular uptake and P-gp/MDR1 (encoded by *ABCB1*) in the cellular efflux of telmisartan.[4–7] Telmisartan acyl-glucuronide is a substrate of OATP1B3 and it is eliminated mainly by biliary excretion.[2,8,9]

High interindividual variability exists in the pharmacokinetics of telmisartan and low exposure to telmisartan is associated with poor blood pressure-lowering effect.[10–12] Telmisartan is usually effective with a 40 mg daily dose, but a significant proportion of patients require a higher dose or combination treatment to achieve sufficient blood pressure control.[13] For optimal therapy, it would be important to understand the sources of variability in the response to antihypertensive medication.

[1]Department of Clinical Pharmacology, University of Helsinki and HUS Diagnostic Center, Helsinki University Hospital, Helsinki, Finland; [2]Individualized Drug Therapy Research Program, Faculty of Medicine, University of Helsinki, Helsinki, Finland. *Correspondence: Mikko Niemi (mikko.niemi@helsinki.fi)

Received April 1, 2020; accepted May 19, 2020. doi:10.1002/cpt.1928

There are few previous studies on the associations of genetic variants on the pharmacokinetics of telmisartan with relatively small sample sizes, but comprehensive studies are lacking. In two of the studies, either the *UGT1A3*2* or the *UGT1A1*28* allele was associated with significantly reduced plasma concentrations of telmisartan.[3,14] In addition, one small study suggested an association between the *ABCC2* c.-24C>T (rs717620) single nucleotide variation (SNV) and telmisartan peak plasma concentration (C_{max}).[15] On the other hand, variants in, for example, *CYP2C8*, *CYP2C9*, *UGT2B7*, *SLCO1B3*, *ABCB1*, and *ABCG2* have not been associated with telmisartan pharmacokinetics.[3,14,16,17] The aim of this study was to evaluate how variations in 379 pharmacokinetic genes associate with telmisartan pharmacokinetics.

METHODS

A total of 188 healthy unrelated white Finnish volunteers participated in the study after giving written informed consent. Their health was confirmed by medical history, clinical examination, and laboratory tests. Participants were not on any continuous medication nor were tobacco smokers. The study was approved by the Coordinating Ethics Committee of the Hospital District of Helsinki and Uusimaa (record number 267/13/03/00/2011) and the Finnish Medicines Agency Fimea (EudraCT number 2011-004645-40). Of the participants, 91 were women and 97 men. Their mean ± SD age was 24 ± 4 years, height 174 ± 9 cm, body weight 69 ± 12 kg, and body mass index 22.8 ± 2.6 kg/m^2.

Telmisartan pharmacokinetics and pharmacodynamics

After an overnight fast, each participant ingested a 40 mg dose of telmisartan (Micardis tablet; Boehringer Ingelheim International GmbH, Ingelheim am Rhein, Germany) with 150 mL of water at 8 AM. Standardized meals were served at 4, 7, and 10 hours after telmisartan ingestion. Timed blood samples (4–9 mL each) were collected to light-protected EDTA tubes prior to and 0.5, 1, 1.5, 2, 3, 4, 5, 7, 9, 12, 24, and 48 hours after telmisartan administration. Tubes were immediately placed on ice. Plasma was separated within 30 minutes and stored at −70°C until analysis. Systolic and diastolic blood pressures were measured in a sitting position with an automatic oscillometric blood pressure monitor (Omron Healthcare Europe BV, Hoofddorp, The Netherlands) before and at 4, 12, and 24 hours after telmisartan ingestion. The pharmacodynamic variables, the average change in diastolic and systolic blood pressure, were calculated by dividing the incremental area under the blood pressure-time curve from time 0 to 24 hours with 24 hours.

Telmisartan and telmisartan acyl-(β-D-)glucuronide plasma concentrations were quantified using a Nexera X2 ultra-high-performance liquid chromatograph (Shimadzu, Kyoto, Japan) coupled to a Qtrap 5500 mass spectrometer (ABSciex, Foster City, CA). Plasma samples were pretreated using a Phree phospholipid removal plate (Phenomenex, Torrance, CA) according to the manufacturer's instructions. In brief, plasma and acetonitrile containing the internal standards were mixed in a ratio of 1:5 (v/v), and the mixture was allowed to incubate for 10 minutes at room temperature. The sample mixture was then filtered through the cartridge, diluted with mobile phase (A), and delivered to the ultra-high-performance liquid chromatography system. Telmisartan and telmisartan acyl-glucuronide were separated on a Kinetex Biphenyl (2.6 μm, 2.1 mm × 100 mm; Phenomenex) using a gradient elution. Mobile phase consisted of 10 mM ammonium formate (pH 3.2, adjusted with formic acid) (A) and acetonitrile (B). The mobile phase gradient was a linear ramp from 30% B to 97% B over 1 minute, followed by 0.5 minutes at 97% B on hold, and an equilibration step back to the starting composition. The flow rate and the column temperature were maintained at 350 μL/min and 30°C, and the injection volume was 5 μL. Isotope-labeled analogs served as internal standards for both analytes. The mass spectrometer was operated in a positive polarity mode and the targeted mass-to-charge ratio (m/z) ion transitions were 515–276 and 691–515 for telmisartan and telmisartan acyl-glucuronide. The lower limits of quantification were 0.3 ng/mL and 0.1 ng/mL, respectively. The day-to-day precision values (coefficients of variation) for both compounds were below 15% and accuracy within ± 15%, except for the lower limits of quantification, for which both precision and accuracy were within 20%.

The areas under the plasma concentration-time curve from 0 hours to infinity ($AUC_{0-\infty}$), C_{max}, and the elimination half-life ($t_{1/2}$) values were calculated for telmisartan and telmisartan acyl-glucuronide with standard noncompartmental methods using Phoenix WinNonlin, version 6.3 (Certara, Princeton, NJ).

DNA sequencing and genotyping

Genomic DNA was extracted from EDTA blood samples using the Maxwell 16 LEV Blood DNA Kit on a Maxwell 16 Research automated nucleic acid extraction system (Promega, Madison, WI). A total of 379 pharmacokinetic genes, comprising phase I and II metabolizing enzymes, influx and efflux drug transporters, and regulatory proteins, were selected to be studied.[18–20] These genes ± 20 kb, were completely sequenced in the study participants using targeted massive parallel sequencing at the Technology Centre at Institute for Molecular Medicine Finland (Helsinki, Finland).[21] NEBNext DNA Sample Prep protocol (New England BioLabs, Ipswich, MA) was used for library preparation and the NimbleGen SeqCap EZ Choice protocol (Roche Sequencing, Pleasanton, CA) for target enrichment capture. Sequencing was done on the Illumina HiSeq2000 platform with 100 bp paired-end reads (Illumina, San Diego, CA). Quality control, short read alignment, and variant calling and annotation were carried out using an in-house developed pipeline.[21] Mean coverage depth was 37.2X. Coverage depth ≥ 10X, Hardy–Weinberg equilibrium $P < 3.15 \times 10^{-7}$ (Bonferroni correction), and proportion missing ≤ 0.05 were used as quality thresholds. A total of 46,064 SNVs with minor allele frequency (MAF) ≥ 0.05 passed these criteria and were included in the statistical analysis. In order to verify genotype calls and to supplement missing data, all study participants were genotyped with TaqMan genotyping assays on a QuantStudio 12K Flex Real-Time PCR System for the *UGT1A* rs13401281, rs3821242, rs4663969, rs6715325, rs6431625, rs45449995, rs4148323, and rs3064744 sequence variations (Thermo Fisher Scientific, Waltham, MA).[18,22] Call identity with sequencing data was 99.5% for rs6715325 and 100% for all other SNVs. In case of discordant results, genotypes obtained by sequencing were used in the statistical analysis.

Statistical analysis

The number of participants was estimated to be sufficient to detect an effect size of f^2 larger than 0.2 with two predictors in multiple linear regression analysis, with a power > 80% (Bonferroni corrected α level 1.09×10^{-6}). The data were analyzed with the statistical programs JMP Genomics 8.2 (SAS Institute, Cary, NC) and IBM SPSS 22.0 for Windows (Armonk, NY). The pharmacokinetic variables were logarithmically transformed before analysis.[23] Sex and body weight were tested as demographic covariates for pharmacokinetic data using stepwise linear regression analysis, with P value thresholds of 0.05 for entry and 0.10 for removal. Possible associations of genetic variants with pharmacokinetic variables were investigated using linear regression analysis fixed for significant demographic covariates with a stepwise approach. A Bonferroni corrected P value threshold of 1.09×10^{-6} was used for the 379 gene and thresholds of 0.05 for entry and 0.10 for removal for the candidate gene analysis. Additive coding was used for genetic variants in the 379 gene analysis and both additive and dummy variable coding in the candidate gene analysis. Haplotype computations for *UGT1A* gene were performed with PHASE version 2.1.1.[24,25] Statistical comparisons of proportions were done using the Fisher's exact test. Possible correlation of telmisartan

AUC with the change in blood pressure during 24 hours was investigated using partial correlation analysis controlling for baseline blood pressure. Comparison of the change in blood pressure during 24 hours between genotype scores was investigated with analysis of variance, with baseline blood pressure as a covariate and P value < 0.05 considered statistically significant. Pharmacokinetic data are given as geometric means with geometric coefficients of variation and ranges, geometric SDs, or 90% confidence intervals (CIs). Pharmacodynamic data are given as arithmetic means with 95% CIs and proportions with 95% CIs.

RESULTS

Telmisartan pharmacogenomics

Among the 188 healthy volunteers, the $AUC_{0-\infty}$ and C_{max} of telmisartan varied 49-fold and 31-fold, respectively, and those of telmisartan acyl-glucuronide 18-fold and 17-fold, respectively (**Table 1**). Both telmisartan $AUC_{0-\infty}$ and C_{max} were larger in women than in men. In addition, body weight was a significant covariate for telmisartan C_{max}. When entering both sex and body weight as independent variables in the regression analysis for telmisartan $AUC_{0-\infty}$, sex ($P = 0.005$) but not body weight ($P = 0.405$) remained significantly associated. This indicates that the association of sex is independent of the weight.

In a stepwise linear regression analysis, which tested the associations of 46,064 SNVs with MAF of at least 0.05, the rs6715325 SNV, located between the *UGT1A4* and *UGT1A3* first exons, showed the strongest association with the $AUC_{0-\infty}$ of telmisartan (**Table 2**, **Figure 1**). The $AUC_{0-\infty}$ was 46% ($P = 1.81 \times 10^{-22}$) smaller per copy of the variant allele. Furthermore, the rs2361501 SNV, located after *UGT1A3* first exon, showed the strongest association with telmisartan C_{max}, which was 26% ($P = 4.00 \times 10^{-7}$) smaller per copy of the variant allele. After adjusting for the rs6715325 or rs2361501 variant, no other variants remained associated with telmisartan $AUC_{0-\infty}$ or C_{max} at the Bonferroni corrected significance level. The investigated genetic variants were not significantly associated with the $t_{1/2}$ of telmisartan.

Similar to parent telmisartan, telmisartan acyl-glucuronide C_{max} was significantly associated with intronic SNVs located around *UGT1A3* first exon. The strongest association was observed with four SNVs (rs13401281, rs11891311, rs7564935, and rs11888459) in complete linkage disequilibrium with each other. The C_{max} was 39% ($P = 6.25 \times 10^{-11}$) higher per copy of the variant allele (**Table 2**). After adjusting for any one of these variants, no other variants remained statistically significantly associated with the C_{max}. The investigated variants were not significantly associated with the $AUC_{0-\infty}$ or $t_{1/2}$ of telmisartan acyl-glucuronide. The telmisartan acyl-glucuronide/telmisartan $AUC_{0-\infty}$ ratio also showed the strongest association with a *UGT1A* variant (**Table 2**).

Linkage disequilibrium and haplotype analysis

In order to identify the causative SNVs underlying the association of the top noncoding *UGT1A* SNVs (rs6715325, rs2361501, rs13401281, and rs4663969) with telmisartan pharmacokinetic variables, we next investigated the linkage disequilibrium profile and computed haplotypes across the *UGT1A* gene. This was done for the top noncoding SNVs and the missense and functional variants (MAF ≥ 0.01) of the *UGT1A*s, which metabolize telmisartan *in vitro* (*UGT1A1*, *1A3*, *1A7*, *1A8*, and *1A9*; **Figure 2**).[3] All the top noncoding SNVs were strongly linked with each other as well as with the two *UGT1A3* c.31T>C (p.Trp11Arg, rs3821242) and c.140T>C (p.Val47Ala, rs6431625) missense SNVs, which define the *UGT1A3*2* allele (**Figure 2a**). The top SNVs were also in a relatively strong linkage disequilibrium with the *UGT1A1*28* allele (rs3064744, c.-54_-53insTA, TA6>TA7) and with the *UGT1A7* c.622T>C (p.Trp208Arg, rs11692021) missense SNV.

Altogether, 25 haplotypes were inferred in the haplotype computation (**Figure 2b**). The top noncoding SNVs were present in

Table 1 Pharmacokinetic variables of telmisartan and telmisartan acyl-glucuronide in 188 healthy volunteers and the effects of significant demographic covariates on these variables

Variable	Geometric mean	CV	Range	Demographic covariate	Effect (90% CI)[a]	*P* value	Adjusted R^2
Telmisartan							
C_{max}, ng/mL	35	80%	5.2–165	Body weight Sex	−14.2% (−18.7%, −9.5%) 31.9% (9.5%, 59.0%)	4.01×10^{-6} 0.0150	0.25 0.27
T_{max}, hour[b]	1.5	—	0.5–9	—			
$AUC_{0-\infty}$, ng·hour/mL	308	84%	37–1797	Sex	55.9% (31.7%, 84.6%)	2.26×10^{-5}	0.09
$t_{1/2}$, hour	18	41%	6.7–83	Body weight	−4.2% (−6.8%, −1.6%)	9.41×10^{-3}	0.03
Telmisartan acyl-glucuronide							
C_{max}, ng/mL	4.4	58%	1.2–19.4	Body weight	−10.7% (−13.8%, −7.5%)	2.54×10^{-7}	0.13
T_{max}, hour[b]	0.75	—	0.5–12	—			
$AUC_{0-\infty}$, ng·hour/mL	74	50%	18–318	Body weight	−7.7% (−10.5%, −4.7%)	3.76×10^{-5}	0.08
$t_{1/2}$, hour	20	58%	7.9–94	Sex	18.5% (4.3%, 34.7%)	0.0296	0.02
Telmisartan acyl glucuronide/ telmisartan $AUC_{0-\infty}$ ratio	0.24	73%	0.05–1.4	Sex	−20.1% (−31.7%, −6.7%)	0.018	0.03

$AUC_{0-\infty}$, area under the plasma concentration-time curve from 0 hour to infinity; CI, confidence interval; CV, geometric coefficient of variation; C_{max}, peak plasma concentration; T_{max} concentration peak time; $t_{1/2}$, elimination half-life.
[a]Per 10% increase in body weight; sex: women vs. men. [b]T_{max} data given as median.

Table 2 Results of the stepwise forward linear regression analysis of the effects of 46,064 SNVs in 379 genes on telmisartan pharmacokinetics

Pharmacokinetic variable	dbSNP ID	Gene	Location	Nucleotide change	MAF	Effect[a]			
						Average	90% CI	*P* value	Adjusted R^{2a}
Telmisartan									
$AUC_{0-\infty}$	rs6715325	*UGT1A4*	Intron 1	c.867 + 69081T>C	0.46	−45.6%	−50.3%, −40.5%	1.81×10^{-22}	0.45
C_{max}	rs2361501	*UGT1A3*	Intron 1	c.867 + 51A>T	0.47	−26.0%	−32.7%, −18.7%	4.00×10^{-7}	0.36
$t_{1/2}$	—								
Telmisartan acyl-glucuronide									
$AUC_{0-\infty}$	—								
C_{max}	rs13401281[c]	*UGT1A4*	Intron 1	c.867 + 346T>G	0.40	39.2%	28.6%, 50.6%	6.25×10^{-11}	0.30
$t_{1/2}$	—								
Telmisartan acyl-glucuronide/telmisartan $AUC_{0-\infty}$ ratio	rs4663969	*UGT1A3*	Intron 1	c.867 + 16674C>A	0.46	91.7%	78.1%, 106.3%	1.02×10^{-32}	0.55

$AUC_{0-\infty}$, area under the plasma concentration-time curve from 0 hour to infinity; CI, confidence interval: C_{max}, peak plasma concentration; dbSNP, database-single-nucleotide polymorphism (National Center for Biotechnology Information Short Genetic Variations database); MAF, minor allele frequency; SNV, single nucleotide variation; $t_{1/2}$, elimination half-life.
[a]Per copy of the minor allele. [b]Includes the effect of significant demographic covariant and the top SNV. [c]rs13401281 is in complete linkage disequilibrium with rs11891311, rs7564935, and rs11888459.

haplotypes which contained *UGT1A3*2* or *UGT1A3*3*. In addition, the rs2361501 SNV was present in the same haplotype with *UGT1A3*6*. Altogether, the *UGT1A3*2* allele was present in 10, *UGT1A3*3* in 4, and *UGT1A3*6* in 1 of the 25 inferred haplotypes. The sum of frequencies was 0.39 for the *UGT1A3*2*, 0.061 for *UGT1A3*3*, and 0.019 for the *UGT1A3*6* containing haplotypes. The most frequent haplotype ($n = 98$; MAF 0.26) contained the *UGT1A3*2*, *UGT1A7*3*, and *UGT1A1*28* alleles.

Candidate gene analysis

Due to the risk of false negative associations with the conservative Bonferroni correction in the primary analysis, we next carried out a candidate gene analysis for telmisartan $AUC_{0-\infty}$ without correction for multiple testing. In this analysis, we included missense and functional variants with MAF of ≥ 0.01 in genes suggested to be involved in telmisartan pharmacokinetics (*UGT1A3*, *UGT1A1*, *UGT1A7*, *UGT1A8*, *UGT1A9*, *SLCO1B3*, *SLCO2B1*, *ABCB1*, and *ABCC2*; **Table S1**). In the analysis, *UGT1A3*2* was associated with a 48% ($P = 3.82 \times 10^{-22}$) and *UGT1A3*3* with a 28% ($P = 7.01 \times 10^{-3}$) reduced $AUC_{0-\infty}$ per copy of the allele, and *SLCO1B3* c.767G>C (p.Gly256Ala, rs60140950) with a 22% ($P = 0.0392$) increased telmisartan $AUC_{0-\infty}$ per copy of the minor allele (**Table 3**). Because of linkage disequilibrium throughout the whole *UGT1A* locus, we repeated the candidate gene analysis using the inferred *UGT1A8-1A9-1A7-1A3-1A1* haplotypes with MAF ≥ 0.01 (**Figure 2b**). All the haplotypes, which contained *UGT1A3*2*, were associated with reduced $AUC_{0-\infty}$ of telmisartan (**Table S2**).

Interestingly, the *UGT1A3*2* allele lacked gene-dose effect especially in men and thus the log-additive regression model seemed to overestimate the $AUC_{0-\infty}$ of heterozygous *UGT1A3*2* carriers. We, therefore, repeated the candidate gene analysis with *UGT1A3*2* divided to four dummy variables representing the heterozygous and homozygous men and women. In this analysis, *UGT1A3*2* heterozygosity and homozygosity in men were associated with a 64% ($P = 1.21 \times 10^{-16}$) and 63% ($P = 5.21 \times 10^{-8}$) reduced telmisartan $AUC_{0-\infty}$, respectively (**Table 3**). In women, the *UGT1A3*2* heterozygosity and homozygosity were associated with 57% ($P = 1.54 \times 10^{-11}$) and 72% ($P = 3.31 \times 10^{-15}$) reduced $AUC_{0-\infty}$, respectively. Entering body weight as a covariate in addition to sex did not change the results.

To further investigate the roles of UGT variants in telmisartan glucuronidation, we next carried out a candidate gene analysis for telmisartan acyl-glucuronide/telmisartan $AUC_{0-\infty}$ ratio with *UGT1A3*2* dummy variables and other *UGT1A3* and *UGT1A1*, *UGT1A7*, *UGT1A8*, and *UGT1A9* variants. *UGT1A3*2* heterozygosity and homozygosity in men were associated with a 177% ($P = 3.13 \times 10^{-27}$) and 293% ($P = 2.25 \times 10^{-18}$) increased telmisartan acyl-glucuronide/telmisartan $AUC_{0-\infty}$ ratio, respectively (**Table S3**). In women, the *UGT1A3*2* heterozygosity and homozygosity were associated with 116% ($P = 8.59 \times 10^{-16}$) and 250% ($P = 1.19 \times 10^{-21}$) increased telmisartan acyl-glucuronide/telmisartan $AUC_{0-\infty}$ ratio, respectively.

To predict telmisartan $AUC_{0-\infty}$ in men and women with different combinations of *UGT1A3* and *SLCO1B3* genotypes, we calculated genotype scores (GS) using the *UGT1A3*2* dummy

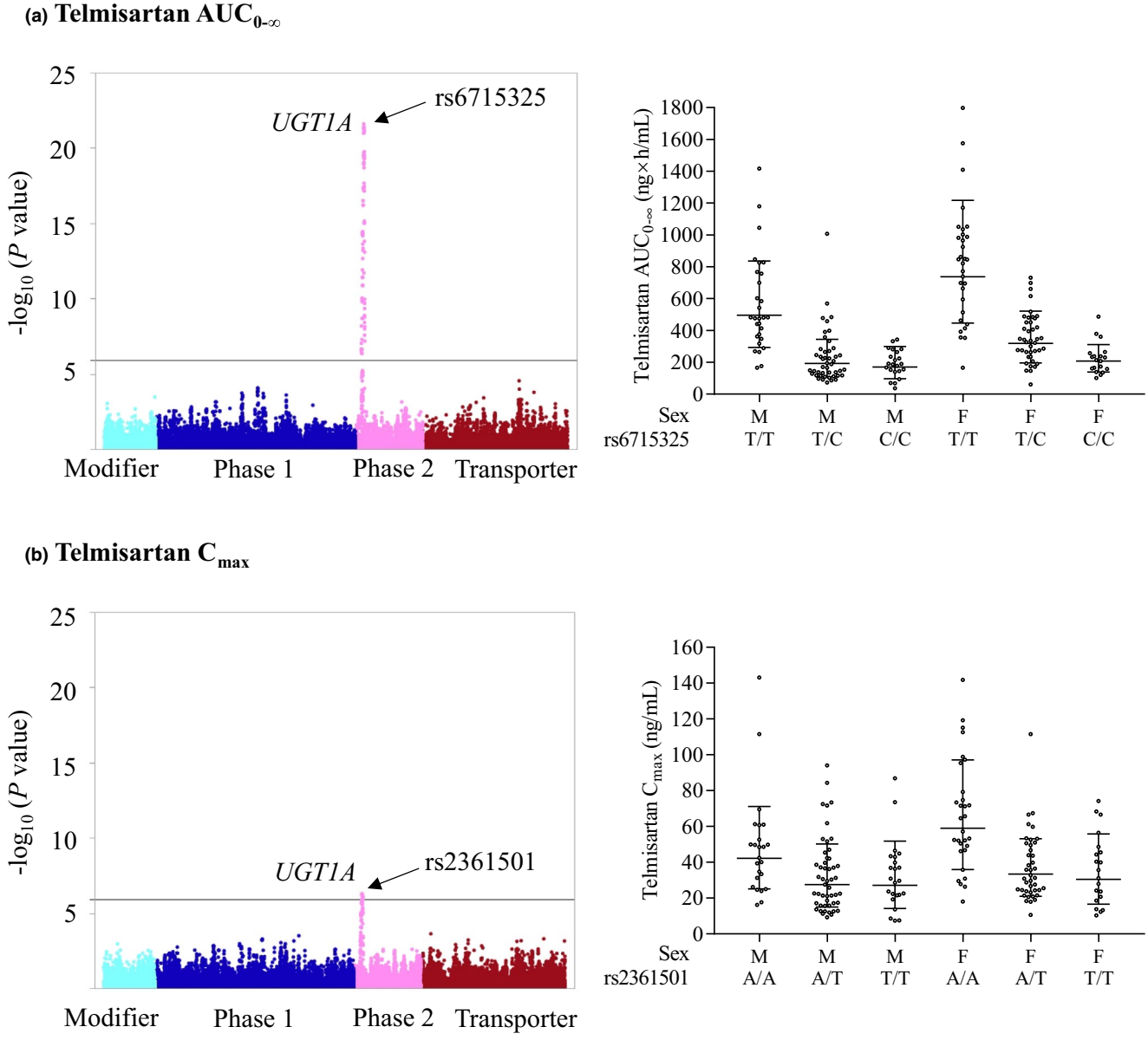

Figure 1 The associations of 46,064 SNVs in 379 pharmacokinetic genes with telmisartan (**a**) area under the plasma concentration-time curve from zero hours to infinity ($AUC_{0-\infty}$) adjusting for sex and (**b**) the peak plasma concentration (C_{max}) adjusting for sex and body weight (left panel). The *Y*-axes describe the negative logarithm of the *P* value for each single nucleotide variation (SNV) and the horizontal lines indicate the Bonferroni corrected significance level of 1.09×10^{-6}. The *X*-axes show individual SNVs grouped by protein function. The geometric mean ± geometric SD $AUC_{0-\infty}$ and body weight adjusted C_{max} values grouped by sex and the top *UGT1A* SNVs rs6715325 and rs2361501 (right panel). [Colour figure can be viewed at wileyonlinelibrary.com]

variable candidate gene linear regression model with the following equation:

$$GS_{telmisartan} = 1.47^{0(M) \text{ or } 1(F)} \times UGT1A3*2 \text{ factor} \times 0.74^{n(UGT1A3*3)} \times 1.23^{n(SLCO1B3c.767G>C)}$$

Where M is male and F is female, *UGT1A3*2* factor is 0.36 for heterozygous men, 0.37 for homozygous men, 0.42 for heterozygous women, 0.28 for homozygous women, and 1 for noncarriers of *UGT1A3*2*, and *n* is the number of variant alleles (0, 1, or 2) of *UGT1A3*3* and *SLCO1B3* c.767G>C (**Figures 3** and **4**). The GS is 1.00 in men who do not carry any of the variants. For others, the score shows the fold difference in telmisartan $AUC_{0-\infty}$ compared with 1.00.

Pharmacodynamics

A total of 65% and 23% of individuals with GS of below 0.5 and between 0.5 and 0.8 had $AUC_{0-\infty}$ values below 229 ng·hour/mL, which was found in a previous study to be the $AUC_{0-\infty}$ value giving 50% of telmisartan maximum effect (**Figure 3**).[12] The respective percentages in individuals with GS between 0.8 and 1.25, and above 1.25 were 6% and 3%. Diastolic blood pressure decreased 1.3 mmHg (95% CI, 0.05, 2.5 mmHg) less in individuals

(a)

	UGT1A8 c.518C>G; p.Ala173Gly; rs1042597	*UGT1A8* c.830G>A; p.Cys277Tyr; rs17863762	*UGT1A9* c.98T>C; p.Met33Thr; rs72551330	*UGT1A7* c.352G>T; p.Asp118Tyr; rs140814031	*UGT1A7* c.386A>G; p.Asn129Ser; rs56385016	*UGT1A7* c.387T>G ; p.Asn129Lys rs17868323	*UGT1A7* c.392G>A ; p.Arg131Gln; rs17868324	*UGT1A7* c.622T>C; p.Trp208Arg; rs11692021	*UGT1A4*; c.867+346T>G; rs13401281	*UGT1A4*; c.867+6908T>C; rs6715325	*UGT1A3* c.31T>C; p.Trp11Arg; rs3821242	*UGT1A3* c.140T>C; p.Val47Ala; rs6431625	*UGT1A3* c.808A>G; p.Met270Val; rs45449995	*UGT1A3*; c.867+51A>T; rs2361501	*UGT1A3*; c.867+16674C>A; rs4663969	*UGT1A1* c.-54_-53insTA; TA6>TA7; rs3064744	*UGT1A1* c.211G>A; p.Gly71Arg; rs4148323
UGT1A8 c.518C>G	-	0.43	$10^{-2.8}$	0.19	0.87	$10^{-7.8}$	$10^{-7.9}$	$10^{-9.4}$	$10^{-7.5}$	$10^{-2.8}$	$10^{-3.2}$	$10^{-8.1}$	0.76	$10^{-3.4}$	$10^{-2.8}$	$10^{-4.7}$	0.58
UGT1A8 c.830G>A	<0.01	-	0.86	0.81	0.86	0.48	0.50	0.10	0.08	0.12	0.13	0.09	0.84	0.13	0.12	0.34	0.75
UGT1A9 c.98T>C	0.052	<0.01	-	0.76	0.82	0.24	0.24	0.14	0.16	0.11	0.10	0.15	0.08	0.1	0.11	0.18	0.70
UGT1A7 c.352G>T	<0.01	<0.01	<0.01	-	0.76	0.11	0.11	$10^{-2.3}$	$10^{-2.5}$	$10^{-2.1}$	0.01	$10^{-2.3}$	0.74	0.01	0.01	$10^{-2.5}$	0.30
UGT1A7 c.386A>G	<0.01	<0.01	<0.01	<0.01	-	0.38	0.40	0.04	0.03	0.36	0.06	0.04	0.81	0.06	0.05	0.02	0.70
UGT1A7 c.387T>G	0.17	<0.01	<0.01	0.014	<0.01	-	10^{-42}	10^{-14}	10^{-12}	10^{-15}	10^{-17}	10^{-13}	0.21	10^{-17}	10^{-16}	$10^{-8.6}$	0.05
UGT1A7 c.392A>G	0.17	<0.01	<0.01	0.013	<0.01	1.00	-	10^{-14}	10^{-12}	10^{-15}	10^{-16}	10^{-13}	0.21	10^{-16}	10^{-15}	$10^{-8.4}$	0.04
UGT1A7 c.622T>C	0.21	0.015	0.012	0.041	0.022	0.33	0.33	-	10^{-24}	10^{-17}	10^{-21}	10^{-27}	0.03	10^{-21}	10^{-18}	10^{-19}	$10^{-2.5}$
UGT1A4 c.867+346T>G	0.16	0.017	0.010	0.047	0.025	0.27	0.27	0.57	-	10^{-32}	10^{-31}	10^{-39}	0.13	10^{-31}	10^{-33}	10^{-27}	0.01
UGT1A4 c.867+6908T>C	0.052	0.013	0.013	0.037	<0.01	0.35	0.35	0.40	0.77	-	10^{-38}	10^{-29}	0.09	10^{-38}	10^{-42}	10^{-20}	0.01
UGT1A3 c.31T>C	0.061	0.012	0.014	0.034	0.018	0.38	0.38	0.48	0.72	0.92	-	10^{-33}	0.05	10^{-42}	10^{-39}	10^{-24}	$10^{-2.4}$
UGT1A3 c.140T>C	0.18	0.016	0.011	0.043	0.023	0.30	0.29	0.64	0.93	0.69	0.78	-	0.02	10^{-33}	10^{-30}	10^{-30}	0.01
UGT1A3 c.808A>G	<0.01	<0.01	0.016	<0.01	<0.01	<0.01	<0.01	0.026	0.012	0.015	0.021	0.027	-	0.04	0.09	0.01	0.67
UGT1A3 c.867+51A>T	0.067	0.012	0.014	0.034	0.019	0.38	0.38	0.48	0.73	0.92	1.00	0.79	0.022	-	10^{-39}	10^{-24}	$10^{-2.4}$
UGT1A3 c.867+16674C>A	0.052	0.013	0.013	0.037	0.020	0.36	0.35	0.41	0.78	0.99	0.93	0.70	0.016	0.93	-	10^{-21}	$10^{-2.2}$
UGT1A1 c.-54_-53insTA	0.10	<0.01	0.010	0.049	0.029	0.20	0.20	0.48	0.67	0.50	0.60	0.76	0.034	0.61	0.51	-	0.36
UGT1A1 c.211G>A	<0.01	<0.01	<0.01	<0.01	<0.01	0.021	0.022	0.046	0.032	0.041	0.045	0.035	<0.01	0.044	0.041	0.032	-

P value

r^2

r^2
1.00
0.90-0.99
0.70-0.90
0.50-0.70
0.30-0.50
<0.30

(b)

haplotype number	*UGT1A8* c.518C>G; p.Ala173Gly; rs1042597	*UGT1A8* c.830G>A; p.Cys277Tyr; rs17863762	*UGT1A9* c.98T>C; p.Met33Thr; rs72551330	*UGT1A7* c.352G>T; p.Asp118Tyr; rs140814031	*UGT1A7* c.386A>G; p.Asn129Ser; rs56385016	*UGT1A7* c.387T>G ; p.Asn129Lys rs17868323	*UGT1A7* c.392G>A ; p.Arg131Gln; rs17868324	*UGT1A7* c.622T>C; p.Trp208Arg; rs11692021	*UGT1A4*; c.867+346T>G; rs13401281	*UGT1A4*; c.867+6908T>C; rs6715325	*UGT1A3* c.31T>C; p.Trp11Arg; rs3821242	*UGT1A3* c.140T>C; p.Val47Ala; rs6431625	*UGT1A3* c.808A>G; p.Met270Val; rs45449995	*UGT1A3*; c.867+51A>T; rs2361501	*UGT1A3*; c.867+16674C>A; rs4663969	*UGT1A1* c.-54_-53insTA; TA6>TA7; rs3064744	*UGT1A1* c.211G>A; p.Gly71Arg; rs4148323	*n*	frequency	*UGT1A8* allele	*UGT1A9* allele	*UGT1A7* allele	*UGT1A3* allele	*UGT1A1* allele
1	C	G	T	G	A	T	G	T	T	T	T	T	A	A	C	TA6	G	57	15.2%					
2	C	G	T	G	A	G	A	T	T	T	T	T	A	A	C	TA6	G	55	14.6%			*2		
3	G	G	T	G	A	T	G	T	T	T	T	T	A	A	C	TA6	G	53	14.1%	*2*				
4	C	G	T	G	A	G	A	C	T	T	T	T	A	A	C	TA6	A	16	4.3%			*3*		*6*
5	G	G	C	G	A	G	A	T	T	T	T	T	A	A	C	TA6	G	6	1.6%	*2*	*3*	*2*		
6	G	G	T	G	A	G	A	T	T	T	T	T	A	A	C	TA6	G	4	1.1%	*2*		*2*		
7	G	G	T	G	A	T	G	T	T	T	T	T	A	A	C	TA7	G	3	0.8%	*2*				*28*
8	C	G	T	G	A	G	A	C	T	T	T	T	A	A	C	TA6	G	2	0.5%			*3*		
9	G	G	T	G	A	T	G	T	T	T	T	T	A	A	C	TA6	A	2	0.5%	*2*				*6*
10	G	G	T	G	A	G	A	C	T	T	T	T	A	A	C	TA6	G	1	0.3%	*2*		*3*		
11	C	G	T	G	A	G	A	C	G	C	C	C	A	T	A	TA7	G	98	26.1%			*3*	*2*	*28*
12	C	G	T	G	A	G	A	C	G	C	C	C	A	T	A	TA6	G	13	3.5%			*3*	*2*	
13	C	G	T	T	A	G	A	C	G	C	C	C	A	T	A	TA7	G	11	2.9%			*15*	*2*	*28*
14	C	G	T	G	A	G	A	T	G	C	C	C	A	T	A	TA7	G	10	2.7%			*2*	*2*	*28*
15	C	G	T	G	G	G	A	C	G	C	C	C	A	T	A	TA7	G	5	1.3%			*10*	*2*	*28*
16	C	A	T	G	A	G	A	C	G	C	C	C	A	T	A	TA6	G	4	1.1%	*3*		*3*	*2*	
17	G	G	T	G	A	G	A	T	G	C	C	C	A	T	A	TA7	G	2	0.5%	*2*		*2*	*2*	*28*
18	C	G	T	G	A	G	A	T	G	C	C	C	A	T	A	TA6	G	2	0.5%			*2*	*2*	
19	C	G	T	G	G	G	A	C	G	T	C	C	A	T	A	TA7	G	1	0.3%			*10*	*2*	*28*
20	C	G	T	G	A	T	G	T	G	C	C	C	A	T	A	TA7	G	1	0.3%				*2*	*28*
21	G	G	T	G	A	G	A	T	T	C	C	T	A	T	A	TA6	G	17	4.5%	*2*		*2*	*3*	
22	C	G	T	G	A	G	A	T	T	C	C	T	A	T	A	TA6	G	4	1.1%			*2*	*3*	
23	C	G	T	G	A	G	A	C	T	C	C	T	A	T	A	TA6	G	1	0.3%			*3*	*3*	
24	G	G	T	G	A	G	A	T	T	C	C	T	A	T	A	TA7	G	1	0.3%	*2*		*2*	*3*	*28*
25	C	G	T	G	A	G	A	C	T	T	C	C	G	T	C	TA7	G	7	1.9%			*3*	*6*	*28*

Figure 2 (**a**) Linkage disequilibrium of the top noncoding SNVs and missense and functional variants of the *UGT1A*s, which metabolize telmisartan *in vitro*. (**b**) *UGT1A* haplotypes inferred with missense and functional variants, and top noncoding *UGT1A* SNVs. Intronic variations are depicted in blue and missense variations in red. The *-alleles are defined on the basis of missense variations within each *UGT1A* enzyme. The *UGT1A7* allele containing the c.352G>T (p.Asp118Tyr, rs140814031) SNV together with c.387T>G, c.392G>A, and c.622T>C SNVs has not been named before and is here given tentatively the name *UGT1A7*15*.[49,50] For clarity, only rs13401281 of the four completely linked telmisartan acyl-glucuronide peak plasma concentration (C_{max}) top SNVs (rs13401281, rs11891311, rs7564935, and rs11888459) is presented in this figure. MAF, minor allele frequency; SNV, single-nucleotide variation. [Colour figure can be viewed at wileyonlinelibrary.com]

Table 3 Results of the candidate gene analyses on telmisartan $AUC_{0-\infty}$

Pharmacokinetic variable	Covariate/SNV	Effect[a]		*P* value	Adjusted R^2 for each step
		Average (%)	90% CI		
Telmisartan $AUC_{0-\infty}$	Sex	58.6	38.3, 81.9	9.79×10^{-8}	0.087
(Log-additive model)	*UGT1A3*2*	−48.5	−53.2, −43.2	3.82×10^{-22}	0.447
	*UGT1A3*3*	−28.2	−41.2, −12.2	7.01×10^{-3}	0.464
	SLCO1B3 c.767G>C (rs60140950)	21.7	4.1, 42.4	0.0392	0.475
Telmisartan $AUC_{0-\infty}$	Sex	47.2	20.6, 79.7	1.58×10^{-3}	0.087
(*UGT1A3*2* dummy variables)	*UGT1A3*2* heterozygous men	−63.6	−69.6, −56.3	1.21×10^{-16}	0.227
	*UGT1A3*2* homozygous women	−71.6	−77.7, −63.9	3.31×10^{-15}	0.321
	*UGT1A3*2* heterozygous women	−57.3	−64.9, −48.1	1.54×10^{-11}	0.439
	*UGT1A3*2* homozygous men	−63.2	−72.5, −50.8	5.21×10^{-8}	0.505
	*UGT1A3*3*	−25.8	−38.2, −11.0	7.47×10^{-3}	0.519
	SLCO1B3 c.767G>C (rs60140950)	23.1	6.7, 42.0	0.0172	0.532

$AUC_{0-\infty}$, area under the plasma concentration-time curve from zero hour to infinity; CI, confidence interval; SNV, single nucleotide variation
[a]Per minor allele copy or per dummy variable; sex: women vs. men.

with GS below 0.8 than in those with GS above 0.8 ($P = 0.042$; **Figure 3**). The average change in systolic blood pressure was not significantly associated with the GS (data not shown). Telmisartan $AUC_{0-\infty}$ correlated negatively with the average change in diastolic ($r = -0.16$; $P = 0.034$) and systolic blood pressures ($r = -0.19$; $P = 0.008$).

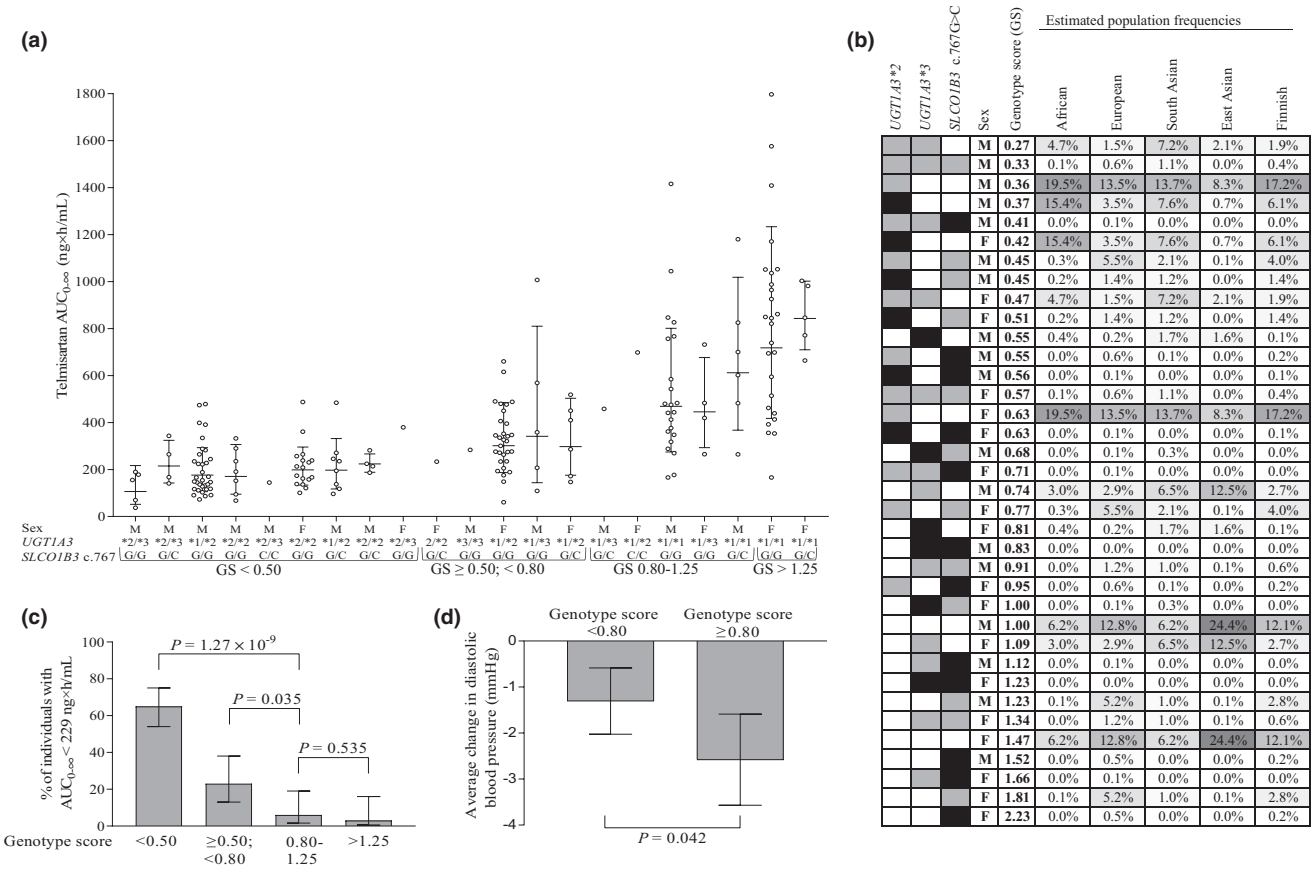

UGT1A3*2	UGT1A3*3	SLCO1B3 c.767G>C	Sex	Genotype score (GS)	African	European	South Asian	East Asian	Finnish
			M	**0.27**	4.7%	1.5%	7.2%	2.1%	1.9%
			M	**0.33**	0.1%	0.6%	1.1%	0.0%	0.4%
			M	**0.36**	19.5%	13.5%	13.7%	8.3%	17.2%
			M	**0.37**	15.4%	3.5%	7.6%	0.7%	6.1%
			M	**0.41**	0.0%	0.1%	0.0%	0.0%	0.0%
			F	**0.42**	15.4%	3.5%	7.6%	0.7%	6.1%
			M	**0.45**	0.3%	5.5%	2.1%	0.1%	4.0%
			M	**0.45**	0.2%	1.4%	1.2%	0.0%	1.4%
			F	**0.47**	4.7%	1.5%	7.2%	2.1%	1.9%
			F	**0.51**	0.2%	1.4%	1.2%	0.0%	1.4%
			M	**0.55**	0.4%	0.2%	1.7%	1.6%	0.1%
			M	**0.55**	0.0%	0.6%	0.1%	0.0%	0.2%
			M	**0.56**	0.0%	0.1%	0.0%	0.0%	0.1%
			F	**0.57**	0.1%	0.6%	1.1%	0.0%	0.4%
			F	**0.63**	19.5%	13.5%	13.7%	8.3%	17.2%
			F	**0.63**	0.0%	0.1%	0.0%	0.0%	0.1%
			M	**0.68**	0.0%	0.1%	0.3%	0.0%	0.0%
			F	**0.71**	0.0%	0.1%	0.0%	0.0%	0.0%
			M	**0.74**	3.0%	2.9%	6.5%	12.5%	2.7%
			F	**0.77**	0.3%	5.5%	2.1%	0.1%	4.0%
			F	**0.81**	0.4%	0.2%	1.7%	1.6%	0.1%
			M	**0.83**	0.0%	0.0%	0.0%	0.0%	0.0%
			M	**0.91**	0.0%	1.2%	1.0%	0.1%	0.6%
			F	**0.95**	0.0%	0.6%	0.1%	0.0%	0.2%
			F	**1.00**	0.0%	0.1%	0.3%	0.0%	0.0%
			M	**1.00**	6.2%	12.8%	6.2%	24.4%	12.1%
			F	**1.09**	3.0%	2.9%	6.5%	12.5%	2.7%
			M	**1.12**	0.0%	0.1%	0.0%	0.0%	0.0%
			F	**1.23**	0.0%	0.0%	0.0%	0.0%	0.0%
			M	**1.23**	0.1%	5.2%	1.0%	0.1%	2.8%
			F	**1.34**	0.0%	1.2%	1.0%	0.1%	0.6%
			F	**1.47**	6.2%	12.8%	6.2%	24.4%	12.1%
			M	**1.52**	0.0%	0.5%	0.0%	0.0%	0.2%
			F	**1.66**	0.0%	0.1%	0.0%	0.0%	0.0%
			F	**1.81**	0.1%	5.2%	1.0%	0.1%	2.8%
			F	**2.23**	0.0%	0.5%	0.0%	0.0%	0.2%

Figure 3 (**a**) The geometric mean ± geometric SD area under the plasma telmisartan concentration-time curve from zero hours to infinity ($AUC_{0-\infty}$) values grouped by genotype scores (GS). The *UGT1A3*1* allele includes all other *UGT1A3* alleles than *UGT1A3*2* and **3*. (**b**) GS for individuals with different genotype combinations. *UGT1A3* and *SLCO1B3* reference genotypes are depicted with white, heterozygous with gray, and homozygous variant genotypes with black rectangles. The estimated population frequencies of the genotype combinations were obtained from the 1000 Genomes Project Data.[18,48] (**c**) The percentage of individuals (95% confidence interval (CI)) with $AUC_{0-\infty}$ < 229 ng·hour/mL in different GS groups. (**d**) The average change (95% CI) in diastolic blood pressure during 24 hours after telmisartan administration in GS groups < 0.8 and ≥ 0.8.

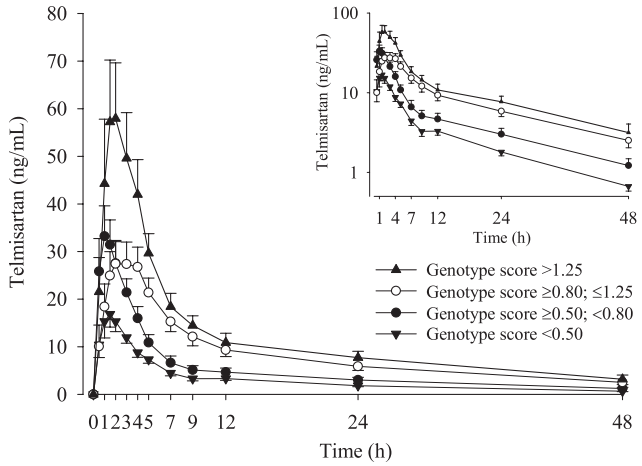

Figure 4 Geometric mean (90% confidence interval (CI)) plasma concentrations of telmisartan after a single 40 mg oral dose of telmisartan in 188 healthy volunteers with different combinations of *UGT1A3* and *SLCO1B3* genotypes. The insets depict the same data on a semilogarithmic scale. The volunteers were grouped according to the genotype score (GS) as follows: GS < 0.50 (n = 80), GS ≥ 0.50; < 0.80 (n = 43), GS ≥ 0.80; ≤ 1.25 (n = 34), and GS > 1.25 (n = 31).

DISCUSSION

In this study, we investigated the associations of variations in 379 genes with telmisartan pharmacokinetics in 188 healthy volunteers. Noncoding variants in the *UGT1A* gene showed the strongest associations with telmisartan pharmacokinetics. These top variants were strongly linked with the *UGT1A3*2* and *UGT1A3*3* alleles, which provides a plausible mechanism for the association. Both *UGT1A3*2* and *UGT1A3*3* were associated with reduced systemic exposure to telmisartan. In addition, a missense variant in *SLCO1B3* was associated with increased telmisartan exposure. Moreover, telmisartan exposure was significantly lower in men than in women. Based on these results, we constructed a scoring system to predict telmisartan plasma exposure in men and women with different combinations of genetic variants.

In this study, the *UGT1A3*2* allele was associated with a markedly reduced telmisartan AUC and explained more than 40% of its interindividual variability. These results are in line with previous studies showing associations between *UGT1A3*2* or linked *UGT1A* variants, such as *UGT1A1*28*, and reduced telmisartan exposure,[3,14,26] and indicate that metabolism via UGT1A3 is the main route of telmisartan elimination. In human liver samples, the *UGT1A3*2* allele has been associated with increased mRNA and protein expression of UGT1A3.[18,27] In addition to telmisartan, the *UGT1A3*2* allele has been associated with increased metabolism of other UGT1A3 substrates, namely montelukast, atorvastatin, and febuxostat.[18,27,28] The causal variant in this haplotype has not yet been identified, however. The haplotype carrying *UGT1A3*2* harbors many noncoding SNVs located around the first exon of *UGT1A3*,[18] which might, for example, influence *UGT1A3* mRNA transcription. Another explanation could be induction of *UGT1A3* expression by bilirubin, whose intrahepatic concentration should be increased in individuals carrying the *UGT1A3*2*-linked *UGT1A1*28*.[3]

In the candidate gene analysis, also the *UGT1A3*3* allele was associated with decreased telmisartan AUC. The effect of this allele was, however, smaller than that of *UGT1A3*2* and explained only 1–2% of the interindividual variability in telmisartan exposure. In previous studies with relatively small numbers of *UGT1A3*3* carriers, the allele has not affected *UGT1A3* mRNA or protein expression in human liver samples.[18,27] *In vitro* studies on the effects of UGT1A3.3 on glucuronidation activity have been inconsistent, with studies showing either reduced or unchanged enzyme activity.[29–31] Given the low allele frequency of *UGT1A3*3* and the relatively weak association with telmisartan exposure, the result needs confirmation in future studies.

In accordance with the associations with parent telmisartan, the *UGT1A3*2* allele was associated with increased telmisartan acyl-glucuronide C_{max} and telmisartan acyl-glucuronide/telmisartan AUC ratio. In theory, the increased metabolite/parent compound AUC ratio could be explained by either increased formation or reduced elimination of the metabolite, or both. Given that the *UGT1A3*2* allele was associated with a reduced AUC and thus an increased oral clearance of telmisartan, increased metabolite formation is the most probable explanation. The increased C_{max} of telmisartan acyl-glucuronide in association with the *UGT1A3*2* allele is likely explained by formation of the metabolite during the first pass. Despite a strong association with the AUC of parent telmisartan, the *UGT1A3*2* allele was not associated with the AUC of the acyl-glucuronide metabolite. This indicates that *UGT1A3*2* increases the rate of glucuronidation of telmisartan, but that the total amount of glucuronide formed is not changed. This is consistent with glucuronidation being the exclusive route of telmisartan elimination.

In addition to UGT1A3, which metabolizes telmisartan with the highest affinity *in vitro*, telmisartan is a substrate of UGT1A1, UGT1A7, UGT1A8, and UGT1A9.[3] All UGT1A enzymes are encoded by the *UGT1A* gene in chromosome 2.[32] They share exons 2–5, but have unique first exons. Strong linkage disequilibrium patterns span the entire *UGT1A* gene.[18] In the present study, we fully sequenced the whole *UGT1A* gene. Of the variants in the other candidate *UGT1A*s, the *UGT1A1*28* and *UGT1A7*3* alleles are strongly linked with *UGT1A3*2*. The *UGT1A1*28* allele has been associated with decreased glucuronidation of *UGT1A1* substrates due to significantly decreased UGT1A1 protein expression.[33–35] Moreover, the *UGT1A7*3* allele has been associated with decreased function of UGT1A7 *in vitro*.[36] After adjusting for the *UGT1A3* effect, no other *UGT1A* variants, including *UGT1A1*28* and *UGT1A7*3*, were significantly associated with telmisartan AUC. Similarly, in the haplotype-based analysis, the *UGT1A1*28* and *UGT1A7*3* alleles did not associate independently with telmisartan pharmacokinetics (**Table S2**). Taken together, these data indicate that genetic variability in UGT1A enzymes other than UGT1A3 is not of major importance for telmisartan pharmacokinetics.

In this study, the *UGT1A3*2* allele seemed to lack a clear gene-dose effect on telmisartan AUC and C_{max}. That is, men showed no difference and women showed only a relatively small difference between *UGT1A3*2* homozygotes and heterozygotes. No obvious explanation exists for these findings. However, linkage between

*UGT1A3*2* and *UGT1A1*28* and a role of UGT1A1 in intestinal telmisartan metabolism may play a role. It is notable, that the effects of the *UGT1A1*28* allele are generally much more pronounced in homozygotes than in heterozygotes,[33–35] whereas those of *UGT1A3*2* are usually seen already in heterozygotes.[18,27] In theory, the effects of *UGT1A1*28* might thus counteract the effects of *UGT1A3*2* on telmisartan pharmacokinetics in *UGT1A3*2/*2–UGT1A1*28/*28* homozygotes.

Considering that telmisartan pharmacokinetics strongly depends on UGT1A3 activity, it could be susceptible to UGT1A3-mediated drug-drug interactions. Interestingly, nisoldipine has increased the AUC of telmisartan by 132%.[37] In human liver microsomes, nisoldipine inhibits the glucuronidation of estradiol,[38] mediated by UGT1A1, UGT1A3, UGT1A8, UGT1A10, and UGT2B7.[39] Further studies are required to determine whether nisoldipine inhibits UGT1A3. Telmisartan could be a useful index substrate for UGT1A3-mediated drug-drug interactions.

Telmisartan has been suggested to be a relatively selective substrate of OATP1B3, an influx transporter expressed on the basolateral membrane of hepatocytes.[4] In the candidate gene analysis, the *SLCO1B3* c.767G>C missense SNV was associated with increased telmisartan AUC, with a 22% increase per minor allele copy. However, this SNV explained only 1% of the interindividual variability in telmisartan exposure. There seems to be no previous studies investigating the associations of this SNV with telmisartan or other OATP1B3 substrate pharmacokinetics in humans. The SIFT and PolyPhen *in silico* prediction tools suggest the c.767G>C SNV to be deleterious.[40,41] In one *in vitro* study, however, this SNV did not significantly affect the uptake of the OATP1B3 substrate cholecystokinin-8.[42] A recent *in vitro* study suggested that OATP2B1 would play a more important role than OATP1B3 in the hepatic uptake of telmisartan.[5] In our study, SNVs in *SLCO2B1* were not, however, associated with telmisartan pharmacokinetics. The analysis included, for example, the c.601G>A SNV associated previously with 3S,5R-fluvastatin and the c.1457C>T SNV associated previously with 3S,5R-fluvastatin, fexofenadine, and celiprolol pharmacokinetics.[43–45]

In accordance with previous studies,[10,16,26] the AUC and C_{max} of telmisartan were significantly lower in men than in women. Body size did not explain this difference. Our finding that the telmisartan acyl-glucuronide/telmisartan AUC ratio was higher in men than in women suggests that the difference could be due to higher telmisartan glucuronidation capacity in men. Interestingly, no sex difference seemed to exist in telmisartan AUC and C_{max} in individuals homozygous for *UGT1A3*2*.

Telmisartan plasma concentration–time profiles are characterized by a biexponential decline after the C_{max}, with a rapid initial distribution followed by a prolonged terminal elimination phase.[10] Of note, no appreciable drug accumulation occurs during multiple dosing. This suggests that our pharmacokinetic results after a single telmisartan dose can be extrapolated to continuous treatment. However, advanced age, concomitant diseases, and other medications may increase variability in telmisartan pharmacokinetics in patients with hypertension as compared with the healthy volunteers of the present study. Nevertheless, the effects of UGT1A variants seem to be similar in patients with hypertension and healthy volunteers.[26] This suggests that the effects of genetic variants on telmisartan pharmacokinetics in healthy volunteers can be extrapolated to patients with hypertension.

The maximum antihypertensive effect of telmisartan is usually attained within 4–8 weeks after the start of treatment, but some effect can be seen already 3 hours after the first dose in patients with hypertension.[11] In general, the antihypertensive effect of telmisartan is much more pronounced in hypertensive than in normotensive individuals. Nevertheless, in our study in normotensive healthy volunteers, the average change in diastolic and systolic blood pressures correlated negatively with telmisartan AUC. Moreover, a low GS was associated with the weak diastolic blood pressure-lowering effect of telmisartan. One should keep in mind, however, that these pharmacodynamic results should not be directly extrapolated to patients with hypertension. The finding that the average change in systolic blood pressure was not significantly associated with the GS may be explained by greater variation in systolic than diastolic blood pressure.

A previous angiotensin II challenge study in healthy volunteers showed that telmisartan efficacy is concentration-dependent. The telmisartan $AUC_{0-\infty}$ value giving 50% of the maximum effect was estimated to be 229 ng × hour/mL.[12] In the present study, the proportion of individuals having $AUC_{0-\infty}$ values below 229 ng·hour/mL after a 40 mg dose increased along with a decreasing GS. In the treatment of hypertension, the effective dose of telmisartan is usually 40 mg once daily, but a significant proportion of patients require 80 mg daily due to poor efficacy.[13] Because the effect of telmisartan is dose-dependent and concentration-dependent, and there is large variability in telmisartan exposure, it is probable that inadequate efficacy with the 40 mg dose may, in some cases, be due to insufficient plasma concentrations. On the other hand, although telmisartan is usually well-tolerated,[46,47] it is possible that increased exposure predisposes to hypotension or other adverse effects. The GS might aid in finding the right telmisartan doses for patients with hypertension.

The participants of this study were white Finnish volunteers, among whom the allele frequency of *UGT1A3*2* was 0.39. The *UGT1A3*2* allele is generally very common in European (0.32), Sub-Saharan African (0.56), and South-Asian (0.42) populations, but less common in East Asians (0.12).[18] On the contrary, *UGT1A3*3* is more common in South and East Asians (MAF 0.20 and 0.18) as compared with Europeans (0.07) and Sub-Saharan Africans (0.086). These interethnic differences in *UGT1A3* allele frequencies lead to differences in the distributions of telmisartan GSs among populations (**Figure 3**).[18,48] In previous studies in Asian individuals, the *UGT1A3*2* allele or linked *UGT1A* variants have been associated with a similar effect on telmisartan pharmacokinetics, as was seen in the present study.[3,14,26] This suggests that our findings can be extrapolated to other populations.

In conclusion, these results indicate that genetic variants of *UGT1A3* associate strongly with the pharmacokinetics of telmisartan. Due to lower plasma concentrations, carriers of *UGT1A3*2* may be at an increased risk of poor blood pressure-lowering efficacy of telmisartan. The results also suggest an association of *SLCO1B3* c.767G>C variant with telmisartan

exposure. The generated GS may aid in individualizing treatment with telmisartan.

SUPPORTING INFORMATION

Supplementary information accompanies this paper on the *Clinical Pharmacology & Therapeutics* website (www.cpt-journal.com).

ACKNOWLEDGMENTS

The authors thank Ms. Katja Halme, Ms. Hanna Hyvärinen, Ms. Satu Karjalainen, Mr. Jouko Laitila, Ms. Eija Mäkinen-Pulli, Ms. Raija Nevala, and Ms. Lisbet Partanen for skillful assistance in conducting the clinical pharmacokinetic study, and Mr. Pekka Ellonen and Ms. Maija Lepistö, M.Sc., for the massive parallel sequencing.

FUNDING

This study was supported by grants from the European Research Council (Grant agreement 282106), State funding for university-level health research, the Sigrid Jusélius Foundation (Helsinki, Finland), the Biomedicum Helsinki Foundation (Helsinki, Finland), and the Orion Research Foundation sr (Espoo, Finland).

CONFLICT OF INTEREST

All authors declared no competing interests for this work.

AUTHOR CONTRIBUTIONS

P.H. and M.Ni. wrote the manuscript. P.H., A.T., J.T.B., and M.Ni. designed the research. P.H., A.T., T.L., M.Ne., T.T., M.P.-H., J.T.B., and M.Ni. performed the research. P.H. and M.Ni. analyzed the data.

© 2020 The Authors. *Clinical Pharmacology & Therapeutics* published by Wiley Periodicals LLC on behalf of American Society for Clinical Pharmacology and Therapeutics.

This is an open access article under the terms of the Creative Commons Attribution-NonCommercial License, which permits use, distribution and reproduction in any medium, provided the original work is properly cited and is not used for commercial purposes.

1. Frampton, J.E. Telmisartan: a review of its use in cardiovascular disease prevention. *Drugs* **71**, 651–677 (2011).
2. Stangier, J. *et al*. Absorption, metabolism, and excretion of intravenously and orally administered [14C]telmisartan in healthy volunteers. *J. Clin. Pharmacol.* **40**, 1312–1322 (2000).
3. Yamada, A. *et al*. The impact of pharmacogenetics of metabolic enzymes and transporters on the pharmacokinetics of telmisartan in healthy volunteers. *Pharmacogenet. Genomics* **21**, 523–530 (2011).
4. Ishiguro, N. *et al*. Predominant contribution of OATP1B3 to the hepatic uptake of telmisartan, an angiotensin II receptor antagonist, in humans. *Drug Metab. Dispos.* **34**, 1109–1115 (2006).
5. Izumi, S. *et al*. Relative activity factor (RAF)-based scaling of uptake clearance mediated by organic anion transporting polypeptide (OATP) 1B1 and OATP1B3 in human hepatocytes. *Mol. Pharm.* **15**, 2277–2288 (2018).
6. Chang, C., Bahadduri, P.M., Polli, J.E., Swaan, P.W. & Ekins, S. Rapid identification of P-glycoprotein substrates and inhibitors. *Drug Metab. Dispos.* **34**, 1976–1984 (2006).
7. Kataoka, M. *et al*. Dynamic analysis of GI absorption and hepatic distribution processes of telmisartan in rats using positron emission tomography. *Pharm. Res.* **29**, 2419–2431 (2012).
8. Ishiguro, N. *et al*. Establishment of a set of double transfectants coexpressing organic anion transporting polypeptide 1B3 and hepatic efflux transporters for the characterization of the hepatobiliary transport of telmisartan acylglucuronide. *Drug Metab. Dispos.* **36**, 796–805 (2008).
9. Maeda, K. *et al*. Quantitative investigation of hepatobiliary transport of [(11)C]telmisartan in humans by PET imaging. *Drug Metab. Pharmacokinet.* **34**, 293–299 (2019).
10. Stangier, J., Su, C.A. & Roth, W. Pharmacokinetics of orally and intravenously administered telmisartan in healthy young and elderly volunteers and in hypertensive patients. *J. Int. Med. Res.* **28**, 149–167 (2000).
11. Smith, D.H., Matzek, K.M. & Kempthorne-Rawson, J. Dose response and safety of telmisartan in patients with mild to moderate hypertension. *J. Clin. Pharmacol.* **40**, 1380–1390 (2000).
12. Stangier, J. *et al*. Inhibitory effect of telmisartan on the blood pressure response to angiotensin II challenge. *J. Cardiovasc. Pharmacol.* **38**, 672–685 (2001).
13. Giles, T.D., Bakris, G.L., Smith, D.H., Davidai, G. & Weber, M.A. Defining the antihypertensive properties of the angiotensin receptor blocker telmisartan by a practice-based clinical trial. *Am. J. Hypertens.* **16**, 460–466 (2003).
14. Ieiri, I. *et al*. Pharmacokinetic and pharmacogenomic profiles of telmisartan after the oral microdose and therapeutic dose. *Pharmacogenet. Genomics* **21**, 495–505 (2011).
15. Miura, M., Satoh, S., Inoue, K., Saito, M., Habuchi, T. & Suzuki, T. Telmisartan pharmacokinetics in Japanese renal transplant recipients. *Clin. Chim. Acta.* **399**, 83–87 (2009).
16. Cabaleiro, T. *et al*. Evaluation of the relationship between sex, polymorphisms in CYP2C8 and CYP2C9, and pharmacokinetics of angiotensin receptor blockers. *Drug Metab. Dispos.* **41**, 224–229 (2013).
17. Guo, X. *et al*. No effect of MDR1 C3435T polymorphism on oral pharmacokinetics of telmisartan in 19 healthy Chinese male subjects. *Clin. Chem. Lab. Med.* **47**, 38–43 (2009).
18. Hirvensalo, P. *et al*. Comprehensive pharmacogenomic study reveals an important role of UGT1A3 in montelukast pharmacokinetics. *Clin. Pharmacol. Ther.* **104**, 158–168 (2018).
19. PharmaADME.org <http://pharmaadme.org>. Accessed May 8, 2020.
20. Morrissey, K.M., Wen, C.C., Johns, S.J., Zhang, L., Huang, S.M. & Giacomini, K.M. The UCSF-FDA TransPortal: a public drug transporter database. *Clin. Pharmacol. Ther.* **92**, 545–546 (2012).
21. Sulonen, A.M. *et al*. Comparison of solution-based exome capture methods for next generation sequencing. *Genome Biol.* **12**, R94 (2011).
22. Ehmer, U. *et al*. Rapid allelic discrimination by TaqMan PCR for the detection of the Gilbert's syndrome marker UGT1A1*28. *J. Mol. Diagn.* **10**, 549–552 (2008).
23. Clinical Pharmacology & Therapeutics Editorial Team. Statistical guide for Clinical Pharmacology & Therapeutics. *Clin. Pharmacol. Ther.* **88**, 150–152 (2010).
24. Stephens, M., Smith, N.J. & Donnelly, P. A new statistical method for haplotype reconstruction from population data. *Am. J. Hum. Genet.* **68**, 978–989 (2001).
25. Stephens, M. & Donnelly, P. A comparison of Bayesian methods for haplotype reconstruction from population genotype data. *Am. J. Hum. Genet.* **73**, 1162–1169 (2003).
26. Pei, Q. *et al*. Effects of genetic variants in UGT1A1, SLCO1B3, ABCB1, ABCC2, ABCG2, ORM1 on PK/PD of telmisartan in Chinese patients with mild to moderate essential hypertension. *Int. J. Clin. Pharmacol. Ther.* **55**, 659–665 (2017).
27. Riedmaier, S. *et al*. UDP-glucuronosyltransferase (UGT) polymorphisms affect atorvastatin lactonization in vitro and in vivo. *Clin. Pharmacol. Ther.* **87**, 65–73 (2010).
28. Lin, M. *et al*. Effects of UDP-glucuronosyltransferase (UGT) polymorphisms on the pharmacokinetics of febuxostat in healthy Chinese volunteers. *Drug Metab. Pharmacokinet.* **32**, 77–84 (2017).
29. Caillier, B. *et al*. A pharmacogenomics study of the human estrogen glucuronosyltransferase UGT1A3. *Pharmacogenet. Genomics* **17**, 481–495 (2007).
30. Chen, Y., Chen, S., Li, X., Wang, X. & Zeng, S. Genetic variants of human UGT1A3: functional characterization and frequency distribution in a Chinese Han population. *Drug Metab. Dispos.* **34**, 1462–1467 (2006).
31. Iwai, M., Maruo, Y., Ito, M., Yamamoto, K., Sato, H. & Takeuchi, Y. Six novel UDP-glucuronosyltransferase (UGT1A3)

polymorphisms with varying activity. *J. Hum. Genet.* **49**, 123–128 (2004).
32. Guillemette, C., Lévesque, É. & Rouleau, M. Pharmacogenomics of human uridine diphospho-glucuronosyltransferases and clinical implications. *Clin. Pharmacol. Ther.* **96**, 324–339 (2014).
33. Monaghan, G., Ryan, M., Seddon, R., Hume, R. & Burchell, B. Genetic variation in bilirubin UPD glucuronosyltransferase gene promoter and Gilbert's syndrome. *Lancet* **347**, 578–581 (1996).
34. Ando, Y., Saka, H., Asai, G., Sugiura, S., Shimokata, K. & Kamataki, T. UGT1A1 genotypes and glucuronidation of SN-38, the active metabolite of irinotecan. *Ann. Oncol.* **9**, 845–847 (1998).
35. Bhatt, D.K. *et al*. Age- and genotype-dependent variability in the protein abundance and activity of six major uridine diphosphate-glucuronosyltransferases in human liver. *Clin. Pharmacol. Ther.* **105**, 131–141 (2019).
36. Guillemette, C., Ritter, J.K., Auyeung, D.J., Kessler, F.K. & Housman, D.E. Structural heterogeneity at the UDP-glucuronosyltransferase 1 locus: functional consequences of three novel missense mutations in the human UGT1A7 gene. *Pharmacogenetics* **10**, 629–644 (2000).
37. Bajcetic, M. *et al*. Pharmacokinetics of oral doses of telmisartan and nisoldipine, given alone and in combination, in patients with essential hypertension. *J. Clin. Pharmacol.* **47**, 295–304 (2007).
38. Satoh, T., Tomikawa, Y., Takanashi, K., Itoh, S., Itoh, S. & Yoshizawa, I. Studies on the interactions between drugs and estrogen. III. Inhibitory effects of 29 drugs reported to induce gynecomastia on the glucuronidation of estradiol. *Biol. Pharm. Bull.* **27**, 1844–1849 (2004).
39. Lépine, J. *et al*. Specificity and regioselectivity of the conjugation of estradiol, estrone, and their catecholestrogen and methoxyestrogen metabolites by human uridine diphospho-glucuronosyltransferases expressed in endometrium. *J. Clin. Endocrinol. Metab.* **89**, 5222–5232 (2004).
40. Sim, N.L., Kumar, P., Hu, J., Henikoff, S., Schneider, G. & Ng, P.C. SIFT web server: predicting effects of amino acid substitutions on proteins. *Nucleic Acids Res.* **40**, W452–W457 (2012).
41. Adzhubei, I.A. *et al*. A method and server for predicting damaging missense mutations. *Nat. Methods* **7**, 248–249 (2010).
42. Schwarz, U.I. *et al*. Identification of novel functional organic anion-transporting polypeptide 1B3 polymorphisms and assessment of substrate specificity. *Pharmacogenet. Genomics* **21**, 103–114 (2011).
43. Hirvensalo, P. *et al*. Enantiospecific pharmacogenomics of fluvastatin. *Clin. Pharmacol. Ther.* **106**, 668–680 (2019).
44. Imanaga, J. *et al*. The effects of the SLCO2B1 c.1457C > T polymorphism and apple juice on the pharmacokinetics of fexofenadine and midazolam in humans. *Pharmacogenet. Genomics* **21**, 84–93 (2011).
45. Ieiri, I. *et al*. Microdosing clinical study: pharmacokinetic, pharmacogenomic (SLCO2B1), and interaction (grapefruit juice) profiles of celiprolol following the oral microdose and therapeutic dose. *J. Clin. Pharmacol.* **52**, 1078–1089 (2012).
46. Stangier, J., Su, C.A., Schöndorfer, G. & Roth, W. Pharmacokinetics and safety of intravenous and oral telmisartan 20 mg and 120 mg in subjects with hepatic impairment compared with healthy volunteers. *J. Clin. Pharmacol.* **40**, 1355–1364 (2000).
47. Manolis, A.J., Reid, J.L., de Zeeuw, D., Murphy, M.B., Seewaldt-Becker, E., Köster, J. & on behalf of the ARAMIS Study Group. Angiotensin II receptor antagonist telmisartan in isolated systolic hypertension (ARAMIS) study: efficacy and safety of telmisartan 20, 40 or 80 mg versus hydrochlorothiazide 12.5 mg or placebo. *J. Hypertens.* **22**, 1033–1037 (2004).
48. Clarke, L. *et al*. The international genome sample resource (IGSR): a worldwide collection of genome variation incorporating the 1000 Genomes Project data. *Nucleic Acids Res.* **45**, D854–D859 (2017).
49. Whirl-Carrillo, M. *et al*. Pharmacogenomics knowledge for personalized medicine. *Clin. Pharmacol. Ther.* **92**, 414–417 (2012).
50. PharmGKB UGT1A7 haplotypes <https://www.pharmgkb.org/gene/PA37182/haplotype>. Accessed March 10, 2020.